**BIODIVERSITAS**
Volume 26, Number 12, December 2025
Pages: 6513-6522

ISSN: 1412-033X
E-ISSN: 2085-4722
DOI: 10.13057/biodiv/d261248

# Screening and characterization of thermostable α-amylase-producing microbes from Karedhe North Buton Hot Springs, Indonesia

**SARLAN[1], RUGAIYAH A. ARFAH[2], ABDUL KARIM[2], ANITA[1], AHYAR AHMAD[2,3,♥], PAULINA TABA[2], HARNINGSIH KARIM[4], SITI HALIMAH LAREKENG[5,6], DOROTHEA AGNES RAMPISELA[7,8], RUSDINA BTE LADJU[9,10]**

[1]Doctoral Program in Chemistry, Faculty of Mathematics and Natural Sciences, Universitas Hasanuddin. Jl. Perintis Kemerdekaan Km. 10, Makassar 90245, South Sulawesi, Indonesia
[2]Department of Chemistry, Faculty of Mathematics and Natural Sciences, Universitas Hasanuddin. Jl. Perintis Kemerdekaan Km. 10, Makassar 90245, South Sulawesi, Indonesia
[3]Research and Development Center for Biopolymers and Bioproducts, LPPM, Universitas Hasanuddin. Jl. Perintis Kemerdekaan Km. 10, Makassar 90245, South Sulawesi, Indonesia. Tel.: +62-81242298799, Fax.: +62-411-586498, ♥email: ahyarahmad@gmail.com
[4]Department of Pharmacy, School of Pharmacy Yayasan Ma'bulo Sibatang. Jl. Mappala 2 Block D5, No. 10, Makassar 90222, South Sulawesi, Indonesia
[5]Faculty of Forestry, Universitas Hasanuddin. Jl. Perintis Kemerdekaan Km. 10, Makassar 90245, South Sulawesi, Indonesia
[6]Research Collaboration Center for KARST Microbes, BRIN-LPPM, Universitas Hasanuddin. Jl. Perintis Kemerdekaan Km. 10, Makassar 90245, South Sulawesi, Indonesia
[7]Faculty of Agriculture, Universitas Hasanuddin. Jl. Perintis Kemerdekaan Km. 10, Makassar 90245, South Sulawesi, Indonesia
[8]Sago Research and Development Center LPPM, Universitas Hasanuddin. Jl. Perintis Kemerdekaan Km. 10, Makassar 90245, South Sulawesi, Indonesia
[9]Hasanuddin University Medical Research Center, Faculty of Medicine, Universitas Hasanuddin. Jl. Perintis Kemerdekaan Km. 10, Makassar 90245, South Sulawesi, Indonesia
[10]Department of Pharmacology, Faculty of Medicine, Universitas Hasanuddin. Jl. Perintis Kemerdekaan Km. 10, Makassar 90245, South Sulawesi, Indonesia

Manuscript received: 19 November 2024. Revision accepted: 28 December 2025.

**Abstract.** *Sarlan, Arfah RA, Karim A, Anita, Ahmad A, Taba P, Karim H, Larekeng SH, Rampisela DA, Ladju RB. 2025. Screening and characterization of thermostable α-amylase-producing microbes from Karedhe North Buton Hot Springs, Indonesia. Biodiversitas 26: 6513-6522.* This study aimed to screen and characterize thermophilic α-amylase-producing bacteria from samples collected at Karedhe hot springs. A total of 23 bacterial isolates were obtained, where 8 isolates showed amylolytic activity. Amylase activity was assessed by iodine staining, which showed significant starch hydrolysis, indicated by clear zones around bacterial colonies. The results showed that isolate SRL40-1-3 had the largest clear zone (4 cm), while SRL40-2-1 produced a clear zone of 5.1 cm, indicating their potential for efficient starch degradation. Additionally, biochemical tests revealed distinct metabolic profiles, with only SRL40-1-3 able to use citrate as a carbon source. Specifically, isolates SRL40-1-3 and SRL40-2-1 were identified as *Enterobacter* sp. and *Enterobacter hormaechei*, respectively, based on molecular analysis. Further optimization studies showed that the optimal starch and $CaCl_2$ concentrations for enzyme production were 1.25% and 0.12%, respectively, for SRL40-1-3. The optimum fermentation times were 42 h for SRL40-1-3 and 45 h for SRL40-2-1. In line with the results, the characterization of crude enzyme α-amylase showed that the optimum pH for both isolates was pH 6 at 50°C. Aside from pH, the optimum starch concentrations for crude enzyme in SRL40-1-3 and SRL40-2-1 were 0.015% and 0.01%, respectively. These results indicate that thermophilic bacteria from Karedhe hot springs have potential applications in industries requiring efficient starch degradation, such as bioethanol production and food processing.

**Keywords:** α-amylase, *Enterobacter hormaechei*, hot spring, starch, thermophilic bacteria

## INTRODUCTION

Sago (*Metroxylon sagu* Rottb.) is an endemic plant widely distributed in Sulawesi, Maluku, and Papua, playing a crucial role in local food security in Eastern Indonesia. As a plant that thrives in wetlands and swampy areas, sago is a primary carbohydrate source for local communities, particularly because it produces starch in large quantities (Sidiq et al. 2021). Sago has gained popularity over the last 5 years as a local food source and commercial commodity. It also offers ecological benefits by enabling growth on marginal soils unsuitable for other crops and by helping preserve wetland areas. More importantly, the sago plant thrives in swamp habitats with high carbon absorption, serving as an essential crop for mitigating climate change and supporting global food demands (Sidiq et al. 2021).

Sago processing begins with the collection of mature trunks, typically 10-15 years old. The trunk is then processed into starch that can be used to make various food products, including papeda and cakes (Rasyid et al. 2020). Recent studies have also observed the potential of sago for other industrial applications, such as bioenergy and derivative products. Moreover, this is consistent with the global trend towards a bio-economy based on sustainable natural resources (Rasyid et al. 2020; Fetriyuna et al. 2024).

According to previous studies, the growth of sago is essential for food security and has the potential to generate economic opportunities in rural and isolated areas of Sulawesi and Eastern Indonesia (Rasyid et al. 2020; Sidiq

et al. 2021). In the context of global food security, sago offers a more environmentally friendly alternative compared to other staple crops, such as rice and corn, particularly in regions prone to food crises (Wulan 2018; Rasyid et al. 2020).

Expanding sago's potential significantly contributes to solid waste generation during processing. The solid sago waste is a lignocellulosic by-product obtained after sago starch extraction. During processing, flour and solid sago waste are mixed at a 1:6 ratio, which is 6 times higher compared to sago starch. Therefore, accumulated waste, which consists of 60% starch and 14% fiber based on dry weight, with 26% lignin, produces unpleasant odors due to organic acids created during sedimentation (Al-Fakih et al. 2024). To address this challenge, solid sago waste from processing can be treated with α-amylase enzymes to isolate starch for commercial use (Rasyid et al. 2020; Susanto et al. 2024). Because sago waste contains a significant amount of starch, it can serve as a substrate for thermophilic bacteria that produce α-amylase.

The α-amylase is an enzyme that plays a significant role in hydrolyzing starch into simple sugars like maltose and glucose (Zhai et al. 2022). In industry, α-amylase is widely used in sectors such as food, textiles, paper, and bioenergy (Farooq et al. 2021) due to thermal stability, particularly at high temperatures. Thermophilic microorganisms in hot springs produce thermally stable α-amylase (Abdollahi et al. 2020; Benammar et al. 2020).

Isolating α-amylase-producing bacteria from hot springs is a multi-step method. Initially, hot spring water or sediment samples are collected and transported to the laboratory, where bacteria are grown on a medium containing starch as a carbon source to enrich the culture. Thermophilic bacteria are obtained by incubating at high temperatures (40-110°C) (Ulucay et al. 2022). After incubation, the growing bacteria colonies are selected and tested for their enzymatic activity against α-amylase using a starch hydrolysis assay, with iodine staining as an indicator. Bacteria that produce a clear zone on the starch medium indicate the presence of α-amylase activity (Rakaz et al. 2021).

Recent studies have focused on isolating thermostable α-amylase-producing bacteria from hot springs for possible biotechnological applications. The development of bioconversion technology based on this enzyme offers energy-efficient alternatives for industrial processes requiring high temperatures (Rakaz et al. 2021; Yassin et al. 2021). Therefore, the objective of this study was to use solid sago waste as a substrate to investigate and characterize thermophilic bacteria producing thermostable α-amylase in Karedhe hot springs of North Buton. The results may provide the potential to increase the value of sago waste through enzymatic reactions using α-amylase.

## MATERIALS AND METHODS

### Materials

The materials used in this study were water samples, nutrient agar (Himedia), methyl red (Home Science Tools), $H_2O_2$ (viva doria), $I_2$ (emsure), KI (emsure), glucose (Merck), sucrose (Merck), maltose (Himedia), lactose (Enzytec™), crystal violet (Merck), safranin (Merck), alcohol (Merck), Simon citrate agar (Merck), triple iron sugar agar (Merck), gelatin (Merck), and sulfite indole motility medium (Merck).

### Samples collection

Water samples were collected from Karedhe hot springs in North Buton, Southeast Sulawesi (4°46′48″S, 122°58′53″E), on December 2, 2023. The samples were placed in glass bottles inside a cooler and transported to the laboratory for further analysis. Sago waste was obtained from the processing facility in Cialam Village, South Konawe (122°35'30"S, 4°7'30"E), on November 19, 2023. The samples were placed in plastic containers and taken to the laboratory for further study.

### Screening and isolation of amylase enzyme-producing thermophilic bacteria

For isolation, water samples containing thermophilic bacteria were spread onto nutrient agar and incubated at temperatures ranging from 40°C to 65°C. Subsequently, isolates growing at each temperature were further incubated in a selective amylolytic medium (nutrient agar + starch) to assess α-amylase activity. The activity was then assessed by dripping iodine solution to obtain a clear zone (Arfah et al. 2020).

### Characterization of bacterial isolates

*Morphology of bacterial isolates*

Morphological observations of each isolate included colony shape, surface observed from the side, edge from above, and color (Marzuki et al. 2021).

*Characterization by Gram staining*

The 24-hour-old isolate culture was prepared as a smear on a glass slide. The preparation was dried in air and then fixed with a Bunsen burner. The dry preparation was dipped in Gram A solution (crystal violet) for 3 minutes, then rinsed with distilled water, dipped in Gram B solution for 1 minute, then washed with distilled water. Furthermore, it was dripped with a Gram C solution. The preparation was dipped with Gram D solution and left to dry, then dipped with immersion oil to be observed under a microscope with a magnification of 1000× (Dalton and Young 2024).

*Biochemical test of bacterial isolates*

Biochemical tests were performed using Simon citrate agar, catalase, triple sugar iron agar, gelatinase, sulfite, indole, methyl red, Voges-Proskauer, and carbohydrate fermentation (Marzuki et al. 2021).

### Molecular identification of thermophilic bacterial isolates

Molecular identification of α-amylase-producing thermophilic bacteria isolates was determined using the 16S rRNA sequence. The sequencing of the 16S rRNA gene was performed using the Sanger method (Next-Generation Sequencing) to obtain the complete 16S rRNA gene sequence with 63F (5'CAG GCC TAA CAC ATG

CAA GTC 3') as forward primer and 1387R (5'GGG CGG WGT GTA CAA GGC 3') as reverse primer. This was followed by analyzing the 16S rRNA gene sequence using appropriate bioinformatics software, such as BLAST (Basic Local Alignment Search Tool). The software allows comparison of sequences with the GenBank database to identify phylogenetic relationships and bacterial taxonomy (Paul 2023).

**Isolation of starch from sago waste**

One kilogram of sago processing waste was mixed with water and stirred. The mixture was then filtered using a cloth, and the solid waste was squeezed until all the water was removed. Subsequently, solid waste was mixed with approximately 1/3 distilled water, stirred, and squeezed until completely drained to obtain a filtrate. This filtrate was treated with 0.5 N NaOH and allowed to precipitate for 24 h. The liquid and precipitate were separated, and the resulting precipitate was referred to as wet starch. This was followed by drying in an oven for 48 h at 50°C. The sample obtained was ground in a mortar and sieved with a 100 mesh sieve to obtain a powder form (Singla et al. 2020).

**Optimization of α-amylase production**

The optimum conditions for α-amylase production are indicated by the highest activity determined by the DNS (3,5-dinitrosalicylic acid) method.

*Determination of optimum starch concentration*

A 24-hour-old thermophilic bacterial isolate was inoculated into the nutrient broth at 40°C in a shaker incubator for 24 h. Approximately 10% of the inoculum was added to the production medium containing 0.5% to 2.5% starch, and the mixture was incubated in a shaker at 40°C and 200 rpm for 24 h. The mixture was then centrifuged at 3500 rpm for 30 minutes, and the supernatant (filtrate) obtained was the crude α-amylase extract. Each crude enzyme extract was then tested for activity using DNS method (Msarah et al. 2020).

*Determination of optimum $CaCl_2$ concentration*

A 24-hour-old thermophilic bacterial isolate was inoculated into the nutrient broth at 40°C in a shaker incubator for 24 h. Subsequently, 10% of the inoculum was added to the production medium containing the optimum starch concentration and varying concentrations of $CaCl_2$ (0.01% to 0.16%), and the mixture was incubated in a shaker at 40°C and 200 rpm for 24 h. The mixture was centrifuged at 3500 rpm and 4°C for 30 minutes to obtain the supernatant (filtrate) as the crude α-amylase extract. Each crude enzyme extract was then tested for activity using the DNS method (Msarah et al. 2020).

*Determination of optimum fermentation time*

A 24-hour-old thermophilic bacterial isolate was inoculated into the nutrient broth at 40°C in a shaker incubator for 24 h. This was followed by adding 10% of the inoculum to the production medium containing the optimum starch and $CaCl_2$ concentrations, and incubating in a shaker at 40°C and 200 rpm. Enzyme activity was measured every 3 h using the DNS method (Msarah et al. 2020) for 54 h.

**Isolation of α-amylase crude enzyme**

Bacterial isolates were inoculated into a production medium containing 1.25% starch and 0.12% $CaCl_2$ for isolate SRL40-1-3 and 0.75% starch and 0.08% $CaCl_2$ for isolate SRL40-2-1, respectively, and incubated at 40°C for 42 h (SRL40-1-3) and 45 h (SRL40-2-1). The mixture was centrifuged at 3500 rpm at 4°C for 30 minutes to obtain supernatant (filtrate) as the crude extract of α-amylase

**Characterization of α-amylase crude enzyme**

*Effect of pH on enzyme activity*

A total of 25 µL of sago waste starch substrate 1.25% for SRL40-1-3 and 0.75% for SRL40-2-1 was mixed with 25 µL of Crude α-amylase enzyme, 25 µL of acetate buffer/phosphate buffer pH 4-7.5, and vortexed for 10 seconds. Furthermore, the mixture was incubated for 1 hour at 40°C. After incubation, 1.425 mL of $H_2O$ and 1.5 mL of DNS reagent were added, and the mixture was vortexed for 10 seconds. The solution was heated in boiling water for 10 minutes, cooled in cold water, and its absorbance was measured at λmax.

*Effect of substrate concentration on enzyme activity*

A total of 25 µL of sago starch substrate at 0.005%-0.025% was mixed with 25 µL of α-amylase enzyme and 25 µL of acetate buffer and/or phosphate buffer at the optimum pH, and vortexed for 10 seconds. The mixture was incubated for 1 hour at 40°C; after incubation, 1.425 mL of $H_2O$ and 1.5 mL of DNS reagent were added. Furthermore, the mixture was vortexed for 10 seconds, heated in boiling water for 10 minutes, cooled in ice water, and the absorbance was measured at λ-max.

*Effect of temperature on enzyme activity*

A total of 25 µL of 0.015% starch substrate for SRL40-1-3 and 0.01% for SRL40-2-1 was mixed with 25 µL of α-amylase enzyme solution, 25 µL of acetate buffer/ phosphate buffer of optimum pH, incubated at 40, 45, 50, 55, 60°C for 1 hour, after incubation 1.425 mL of $H_2O$ and 1.5 mL of DNS reagent were added. Furthermore, the mixture was vortexed for 10 seconds, heated in boiling water for 10 minutes, cooled in ice water, and the absorbance was measured at λmax.

## RESULTS AND DISCUSSION

**Screening of thermophilic bacteria**

Based on screening and isolation, 23 thermophilic bacterial isolates were successfully obtained from water samples. Among these isolates, 8 were identified as amylase-producing bacteria, comprising 5 from samples incubated at a temperature of 40°C, and 3 isolates were obtained at 45°C, both under a neutral pH of 7. Dripping the iodine method identified bacteria's capacity to hydrolyze starch into simpler sugars like maltose or glucose. The detection procedure included examining the occurrence of a clear

zone surrounding the colonies, indicating starch hydrolysis (Singla et al. 2020).

The results showed that not all isolates had the same level of enzyme activity. Among the 8 amylolytic isolates found from Karedhe hot springs, 2 were selected based on the size of the clear zones produced, indicating their ability to hydrolyze starch. The diameters of hydrolysis zones indicated that isolates had substantial amylase activity. SRL40-1-3 had a clean zone of 4 cm, while SRL40-2-1 showed the largest zone, which measured 5.1 cm (Figure 1). The size of these zones was directly related to each isolate enzymatic effectiveness in breaking down starch. The clear zone identified bacteria showing amylolytic activity, also referred to as a hydrolysis zone, on the agar medium containing 1.0% starch. The size of the clear zone surrounding the colonies varied, showing the different capacities of each isolate to break down starch (Arfah et al. 2020). Bacteria with higher amylolytic activity produced larger hydrolysis zones, suggesting that starch was digested more effectively. This clear zone showed starch breakdown, enabling comparison of the effectiveness of different bacterial isolates. The amount of amylase enzyme activity generated by bacterial isolates is closely proportional to the size of the clear zone. Greater α-amylase secretion by the bacteria or the enzyme's excellent starch-breaking efficiency is indicated by larger clear zones (Mittal et al. 2022).

The screening and isolation operations were carried out under controlled conditions, namely at an incubation temperature of 40°C and a neutral pH of 7, which were optimal for the growth and activity of thermophilic bacteria. Previous studies have shown that amylase-producing microbes such as *Bacillus licheniformis* are isolated at 35 C, pH 7 (Fincan et al. 2021). The constancy of these conditions ensures that the observed variations in clear zone widths are related to the isolates' inherent enzymatic capabilities rather than to external environmental factors.

Thermophilic bacteria producing amylase have also successfully isolated from hot spring such as *Bacillus cereus* from the Hot Spring of Pentadio Resort with 23.26 mm diameter inhibition zone (Angio et al. 2024), *Bacillus amyloliquefaciens* from Nglimut Hot Springs with 2.38 of amylolytic index (Budiharjo et al. 2024) and *Anoxybacillus flavithermus* with 4.24 amylolytic index from Hot Spring Sabah (Fazal et al. 2022).

**Morphological characteristics**

The comparison of isolates and the results of different methods, including the macroscopic appearance of bacterial colonies, is presented in Table 1.

According to Table 1, both isolates are Gram-positive bacteria. This suggests that bacterial cell walls include a strong peptidoglycan coating that preserves the crystal violet stain used in Gram staining. This feature is crucial since Gram-positive bacteria often show different characteristics than Gram-negative, such as a higher resilience to particular environmental stresses and different antibiotic sensitivity.

Regarding motility and flexibility, SRL40-1-3 belonged to spirochete or spirilla-shaped bacteria. Spiral-shaped bacteria are observed for their distinct corkscrew motion, which can be helpful in some conditions, such as thick liquids or mucus, allowing efficient mobility. This form also indicates distinct adaptations or ecological niches, where certain bacteria thrive, particularly in hot springs (Boymurod 2024).

SRL40-2-1 was coccus-shaped bacteria, suggesting a spherical form. The spherical form of SRL40-2-1 may indicate distinct environmental adaptations. Depending on their mode of cellular division, cocci often show in chains (streptococci), clusters (staphylococci), or pairs (diplococci). As shown in thermal springs, superb structural integrity is often connected with coccus-shaped bacteria, which can provide an edge in surviving environmental pressures or higher temperatures (Andriyani et al. 2021). The unique physical and Gram staining properties provide essential information on the 2 isolates' biological identities and possible activities.

**Biochemical characteristics of selected bacterial isolates**

The results of biochemical tests of isolates SRL40-1-3 and SRL40-2-1 are presented in Table 2. Specifically, in Simmons' citrate agar test, SRL40-1-3 showed the ability to use citrate as a carbon source. The medium changes in color from green to blue when the bacteria break down citrate. The blue color indicates that SRL40-1-3 moves and degrades citrate, an essential component of life in environments where it is among the few readily available carbon sources. This metabolic feature suggests that SRL40-1-3 can live in more varied biological settings where different carbon sources, such as citrate, are available, thereby improving its flexibility and utility in biotechnological applications. SRL40-2-1 did not show any color change in the medium, indicating that citrate could not be used as a carbon source in Simon's citrate agar test. The medium stayed green, showing insufficient transport proteins or enzymes for citrate metabolism. This implies that SRL40-2-1 relies on more common carbon sources, including glucose or monosaccharides, for growth and sustenance. The inability to metabolize citrate can influence the environmental conditions under which SRL40-2-1 thrives, limiting its ecological versatility compared to SRL40-1-3.

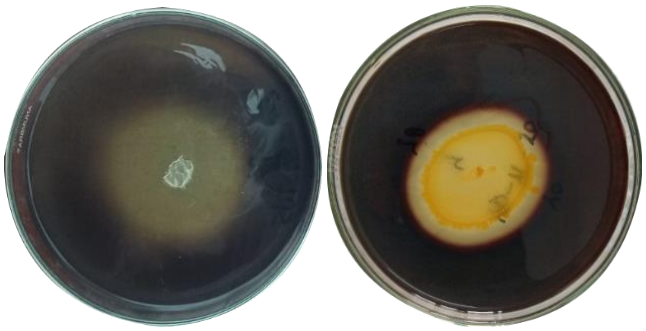

A B

**Figure 1.** Isolates from: A. SRL40-1-3, and B. SRL40-2-1 showed a large diameter of the clear zone after 48 h of incubation at 40°C

**Table 1.** Morphological characteristics of selected bacterial isolates from Karedhe hot spring

| Isolates code | Colony morphology | | | | |
|---|---|---|---|---|---|
| | Colony color | Form | Gram's color | Gram staining | Colony surface |
| SRL40-1-3 | Cream | Spiral | Violet | + | Spread |
| SRL40-2-1 | Cream | Coccus | Violet | + | Spread |

**Table 2.** Morphological characteristics of selected bacterial isolates from Karedhe hot spring

| Biochemical test | Isolates code | |
|---|---|---|
| | SRL40-1-3 | SRL40-2-1 |
| Simon Citrate Agar | + | - |
| Catalase | - | - |
| Triple Sugar Iron Agar | + | + |
| Gelatinase | + | - |
| Motility | + | + |
| Methyl Red | + | - |
| Voges Proskauer | + | - |
| Glucose | + | - |
| Sucrose | + | + |
| Lactose | + | - |
| Maltose | + | + |
| Simon Citrate Agar | + | - |

Note: +: Presence, -: Absence

Both isolates showed a positive reaction in the Triple Sugar Iron (TSI) agar test, which evaluates bacteria's capacity to digest sugars such as glucose, lactose, and sucrose, as well as their ability to produce gas or hydrogen sulfide. The yellow color in both media implies that either isolate can ferment one or more sugars found in the medium. This similar capacity suggests that, despite the different citrate consumption, both SRL40-1-3 and SRL40-2-1 can efficiently metabolize simple sugars. Therefore, SRL40-1-3 and SRL40-2-1 have potential benefits for industrial fermentation processes and bioethanol generation.

The absence of bubble development around the bacterial colonies indicates that no isolates can degrade hydrogen peroxide ($H_2O$) into water ($H_2O$) and oxygen ($O_2$). Effervescence, in the catalase assay, is the breakdown of $H_2O_2$ into oxygen gas under the action of the enzyme catalase. The absence of bubbles suggests that these isolates do not produce catalase, an enzyme in aerobic and facultative anaerobic bacteria that protects against oxidative damage.

In the gelatinase test, a clear difference in enzymatic activity was observed between the 2 isolates. Based on the results, SRL40-1-3 produced a positive result, as the gelatin medium remained liquid after 30 minutes of chilling, verifying the generation of gelatinase. This enzyme catalyzes the breakdown of gelatin into smaller peptides and amino acids, indicating that SRL40-1-3 has proteolytic capacity to degrade surrounding proteins for energy. In comparison, SRL40-2-1 produced a negative result because the gelatin medium hardened following refrigeration, indicating a lack of gelatinase activity. This suggests that SRL40-2-1 relies on other food sources or metabolic pathways. The different gelatinase activity shows the unique enzymatic capacity of various bacterial isolates, which can affect their ecological functions and possible industrial uses, particularly in protein degradation or food recycling procedures.

All bacterial isolates showed motility as determined by the Sulfide Indole Motility (SIM) test. The movement of bacteria inside the media showed that the isolates could efficiently negotiate their surroundings. Motility is essential for bacteria, as it helps them find resources, avoid hostile environments, and establish new habitats.

Aside from the motility assessment, the Methyl Red-Voges-Proskauer (MR-VP) test provided additional information on the isolate's metabolic pathways. The test produced promising results for isolate SRL40-1-3, as shown by developing a purple ring in MR-VP media when 2 drops of methyl red were added. The color shift indicated that SRL40-1-2 could carry out mixed-acid fermentation, generating stable acid end products and reducing the medium pH. In comparison, SRL40-2-1 produced negative results, suggesting no capacity for mixed acid fermentation. The application of barite A and B reagents showed that SRL40-1-3 produced favorable results with a reddish-purple ring, indicating acetoin synthesis through the butylene glycol fermentation route.

Carbohydrate fermentation tests were conducted to assess glucose, sucrose, maltose, and lactose to gauge the metabolic capabilities of bacteria isolates. Sucrose and maltose assays were particularly significant, as all isolates showed promising results after changing the medium to yellow color.

Further analysis of glucose and sucrose tests indicated significant differences in isolates' fermentation capacities. SRL40-1-3 showed positive results in both tests, as indicated by a color change in the medium, suggesting that the sugars were effectively fermented. The metabolic adaptability of SRL40-1-3 showed potential applications across various settings, including glucose and sucrose, which might be beneficial for food processing or fermentation. SRL40-2-1 produced negative results in both tests due to the lack of color change, indicating the inability to ferment sugars. The lack of fermenting capacity can limit the biological niches accessible to SRL40-2-1, underscoring the importance of determining its metabolic properties for potential industrial and environmental applications. The fermentation characteristics of these isolates provide new insights into metabolic pathways and their potential for biotechnological applications.

**Molecular identification of thermophilic bacterial isolates**

Molecular identification of isolates with the greatest antibacterial activity from both areas using particular primers indicated that bacterial isolates belonged to the *Enterobacter* genus. Based on sequencing and BLAST analyses (Tables 3 and 4), SRL40-1-3 was identified as *Enterobacter* sp., and SRL40-2-1 as *Enterobacter hormaechei*. Figure 2 presents the phylogenetic relationships and molecular profiles of the identified isolates. Understanding the specific species within the *Enterobacter* genus is essential, as different species can exhibit distinct pathogenicity and antibacterial activity.

**Table 3.** Blast analysis of isolate SRL40-1-3

| Scientific names | Max score | Total score | Query cover | E value | Per. ident | Acc. len | Accession no. |
|---|---|---|---|---|---|---|---|
| *Enterobacter* sp. | 1882 | 1882 | 99% | 0 | 98.41% | 1524 | OP941830.1 |
| *Enterobacter quasihormaechei* | 1882 | 1882 | 99% | 0 | 98.41% | 1429 | PP067181.1 |
| *Enterobacter* sp. | 1882 | 1882 | 99% | 0 | 98.41% | 1431 | MF289157.1 |
| *Enterobacter hormaechei* subsp. *xiangfangensis* | 1882 | 1882 | 99% | 0 | 98.41% | 1274 | ON038428.1 |
| *Enterobacter kobei* | 1882 | 1882 | 99% | 0 | 98.41% | 1476 | KY287933.1 |
| *Enterobacter cancerogenus* | 1882 | 1882 | 99% | 0 | 98.41% | 1458 | HQ407292.1 |
| *Enterobacter* sp. | 1882 | 1882 | 99% | 0 | 98.41% | 1399 | OR506144.1 |
| *Enterobacter* sp. | 1882 | 1882 | 99% | 0 | 98.41% | 1477 | OK325979.1 |
| *Enterobacter hormaechei* | 1882 | 1882 | 99% | 0 | 98.41% | 1407 | OM181067.1 |
| *Enterobacter cloacae* | 1882 | 1882 | 99% | 0 | 98.41% | 1463 | AB244288.1 |

**Table 4.** Blast analysis of isolate SRL40-2-1

| Scientific names | Max score | Total score | Query cover | E value | Per. ident | Acc. len | Accession no. |
|---|---|---|---|---|---|---|---|
| *Enterobacter hormaechei* | 2025 | 2025 | 99% | 0 | 96.57% | 1417 | PP087077.1 |
| *Enterobacter* sp. | 2023 | 2023 | 96% | 0 | 97.63% | 1219 | OR789349.1 |
| *Enterobacter hormaechei* | 2023 | 2023 | 98% | 0 | 96.87% | 1367 | KC431791.1 |
| *Enterobacter hormaechei* | 2023 | 2023 | 99% | 0 | 96.64% | 1243 | OR229886.1 |
| *Enterobacter* sp. | 2017 | 2017 | 99% | 0 | 96.49% | 1524 | OP941830.1 |
| *Enterobacter quasihormaechei* | 2017 | 2017 | 99% | 0 | 96.49% | 1429 | PP067181.1 |
| *Enterobacter* sp. | 2017 | 2017 | 99% | 0 | 96.49% | 1431 | MF289157.1 |
| *Enterobacter hormaechei* subsp. *xiangfangensis* | 2017 | 2017 | 98% | 0 | 96.71% | 1274 | ON038428.1 |
| *Enterobacter kobei* | 2017 | 2017 | 99% | 0 | 96.49% | 1476 | KY287933.1 |
| *Enterobacter* sp. | 2017 | 2017 | 99% | 0 | 96.49% | 1477 | OK325979.1 |

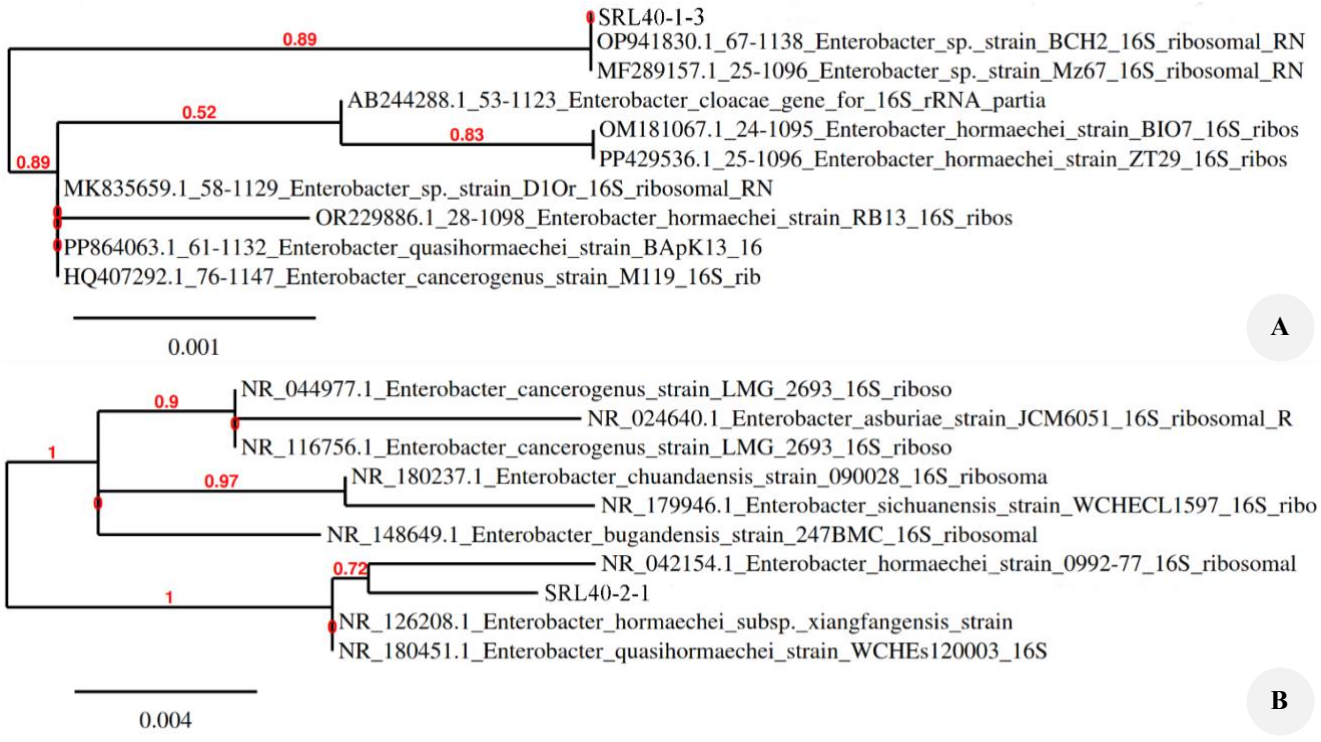


**Figure 2.** Phylogenetic tree construction of both isolates: A. SRL40-1-3, and B. SRL40-2-1

**Separation of starch from sago waste**

The results showed that sago waste contains 19.73% starch, indicating its potential for application despite its neglect in the industry. However, there is a discrepancy when compared to the past study by Susanto et al. (2024), which reports a starch content of approximately 60%. This variation in results can be attributed to differences in methods and sample collections.

Differences in the type of sago investigated, the waste-processing method, or the environmental conditions during waste generation can cause variations in results. Therefore, further studies are recommended to clarify the elements influencing starch concentration in solid sago waste. This study supports previous results and lays the groundwork for developing more effective methods for using sago waste as a starch source, which is relevant across several industrial sectors, including food production, bioenergy, and raw materials for biotechnological products.

**Optimization of α-amylase enzyme production**

*Determination of enzyme activity at the optimum starch concentration*

Figure 3 shows the relationship between starch concentration and α-amylase enzyme activity produced by every isolate. The results show that SRL40-1-3 achieved the optimal starch content of 1.25%, suggesting that α-amylase production was most efficient at this concentration. This suggests that isolate SRL40-1-3 had a better capacity to break down starch at 1.25% due to more favorable enzyme activity or increased substrate availability.

In comparison, SRL40-2-1 shows a lower optimum starch concentration of 0.75%. This isolate produced more α-amylase enzyme at lower starch concentrations than SRL40-1-3. Starch functions as a carbon source and α-amylase enzyme inducer in the growth of amylolytic bacteria, thus affecting bacterial growth and α-amylase production (Arfah et al. 2020). Figure 3 shows a difference in α-amylase production at each starch concentration in the media. The highest α-amylase activity indicates that the optimal concentration of starch to add has been reached. The same case also happened to *Bacillus licheniformis* and *Bacillus subtilis* (Msarah et al. 2020), *B. amyloliquefaciens* (Pham et al. 2021), *B. velezensis* 2% (Bhatt et al. 2020) with optimum starch concentrations of 1%, 1%, and 2%, respectively. The differences in results can be attributed to alterations in each isolate's metabolic pathways and to the efficacy of the enzymes produced. Optimizing substrate concentration maximizes enzyme production, improving the efficiency of biotechnological operations using α-amylase in food, animal feed, and bioenergy industries.

*Determination of enzyme activity on the optimum $CaCl_2$ concentration*

Figure 4 shows the effect of various $CaCl_2$ concentrations on the produced enzyme activity by all isolates. The study found that the optimum $CaCl_2$ concentration for isolate SRL40-1-3 was 0.12%, as shown by the highest enzyme activity. This shows that $CaCl_2$ can operate as a cofactor, increasing enzyme activity and improving metabolic efficiency.

SRL40-2-1 showed an optimum $CaCl_2$ concentration of 0.08%, significantly different from SRL40-1-3. Variation in the result may be due to the alterations in each isolated biological system or metabolic pathway. The addition of calcium ions can increase α-amylase activity (Arfah et al. 2020). This is because calcium ions act as both stabilizers and activators of amylase. The addition of calcium ions after the optimum concentration is reached causes a decrease in amylase enzyme α-activity because too high a calcium concentration can inhibit bacterial growth and α-amylase enzyme production (Arfah et al. 2020; Pham et al. 2021). The addition of $CaCl_2$ to the production of α-amylase enzyme by *B. amyloliquefaciens* was (Pham et al. 2021), *B. atrophaeus* (Abd-Elaziz et al. 2020), *B. tequilensis* (Paul et al. 2020) shows the same trend as the optimum $CaCl_2$ concentrations of 0.02%, 0.02%, and 0.1%, respectively. These data provide insights into how environmental variables might influence enzyme activity and production of each isolate.

*Determination of enzyme activity at the optimum fermentation time*

Figure 5 shows the optimal fermentation time for starch and the relationship between time and α-amylase enzyme output for each strain. After 42 h of fermentation, SRL40-1-3 generates α-amylase with the best efficiency. The short fermentation time indicates that SRL40-1-3 had a faster metabolism or a better capacity to respond to environmental changes, thereby enabling optimal enzyme synthesis.

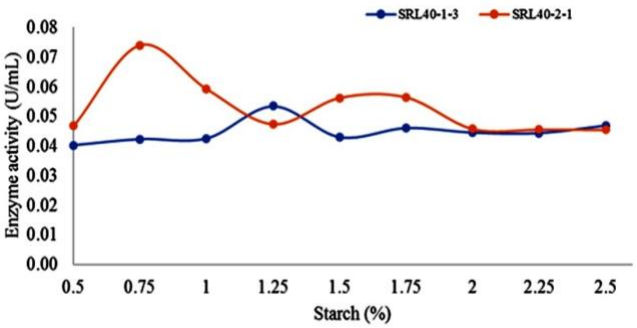


**Figure 3.** Determination of enzyme activity at the optimum starch concentration

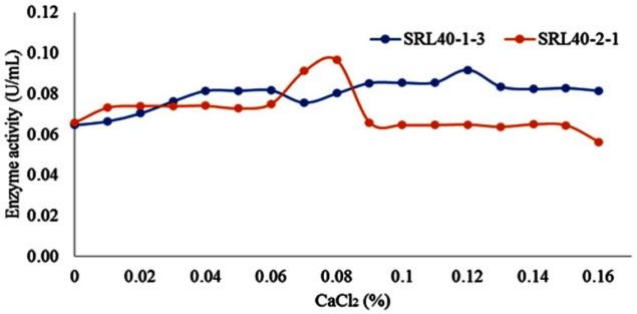


**Figure 4.** Determination of enzyme activity on the optimum $CaCl_2$ concentration

SRL40-2-1 has a slightly longer optimum fermentation time of 45 h. This suggests that SRL40-2-1 will take longer to reach optimal enzyme production levels due to slower cell growth or more effective substrate breakdown. The difference in fermentation time is influenced by various factors related to the biological characteristics of each bacterium and the fermentation environment conditions. Each species or strain of amylolytic bacteria has a different growth rate. Bacteria that grow faster will reach the exponential phase and the enzyme production phase (including amylase) earlier, so that the fermentation time is shorter (Bhatt et al. 2020). Adaptability to the fermentation environment also affects the optimum fermentation time. Some bacteria adapt more quickly to environmental conditions such as oxygen levels, osmotic pressure, or inhibitory compounds. Bacteria that do not adapt soon will take longer to start producing (Pham et al. 2021; Rajesh and Gummadi 2022). This results in a difference in optimal fermentation time between isolates SRL40-1-3 and SRL40-21. Previous studies have also shown differences in fermentation time, even though they come from the same genus, such as *B. licheniformis,* which was 36 h (Fincan et al. 2021), *Bacillus* sp. 48 h (Rajesh and Gummadi 2022), *B. licheniformis* and *B. subtilis* 48 h (Msarah et al. 2020), *B. amyloliquefaciens* 96 h (Pham et al. 2021), *Bacillus velezensis* 86 h (Bhatt et al. 2020). These results provide valuable insights into fermentation dynamics, particularly how each isolate responds to different fermentation conditions.

**Characterization of α-amylase crude enzyme**

*Effect of pH on enzyme activity*

Figure 6 shows the effect of pH on α-amylase activity, indicating the relationship between high pH and α-amylase activity for each isolate.

Figure 6 shows that crude α-amylase enzyme extracts from isolates SRL40-1-3 and SRL40-2-1 exhibit higher activity at high pH, peaking at 6. The pH value can affect α-amylase enzyme activity because enzymes have specific three-dimensional structures that depend on environmental conditions, including pH. α-amylase has an optimum pH of 6-7, where the enzyme is in its most stable and efficient state for catalyzing the reaction. If the pH is too low (acidic), excess hydrogen ions ($H^+$) can disrupt hydrogen bonds and ionic interactions within the enzyme, leading to denaturation or changes in the enzyme's active site that prevent proper substrate binding. Conversely, if the pH is too high (basic), high concentrations of hydroxide ions ($OH^-$) can also damage the enzyme structure and disrupt the charge on important amino acids, thereby reducing or even stopping the enzyme's catalytic activity (Al-Agamy et al. 2021; Balakrishnan et al. 2021). Previous research also showed that the optimum pH of the amylase enzyme ranges from 6-7, such as *B. licheniformis* and *B. subtilis,* which was 6 (Msarah et al. 2020), *Aspergillus oryzae* 6 (Balakrishnan et al. 2021), *B. amyloliquefaciens* 7 (Pham et al. 2021), and *Bacillus* sp. 5 (Rajesh and Gummadi 2022). Beyond the optimal pH, the enzyme's activity tends to decrease due to structural changes or ionization effects. This behavior is similar to α-amylase enzymes from diverse microbial sources, which typically show maximal activity in slightly acidic to neutral pH ranges.

*Effect of substrate concentration on enzyme activity*

Figure 7 shows that the activity of the α-amylase enzyme in crude extracts increases with substrate concentrations. The enzyme activity of SRL40-1-3 peaks at a substrate concentration of 0.015%, while SRL40-2-1 reaches its maximum at 0.01%. Starch concentration can affect the activity of the α-amylase enzyme because the enzyme works by binding the substrate (in this case starch) to its active site to initiate the hydrolysis reaction. If the starch concentration is too low, the number of substrate molecules available to interact with the enzyme is also small, so the reaction rate becomes slow because many enzymes do not work optimally. Conversely, if the starch concentration is too high, all active sites of the enzyme will be quickly saturated by the substrate. Once the saturation point is reached, further addition of starch will not increase the reaction rate because the enzyme has worked at maximum capacity (Bangar et al. 2022; Shen et al. 2022). In addition, too high a substrate concentration can cause an increase in the viscosity of the solution, which can inhibit diffusion and reduce the efficiency of contact between the enzyme and the substrate (Arfah et al. 2020).

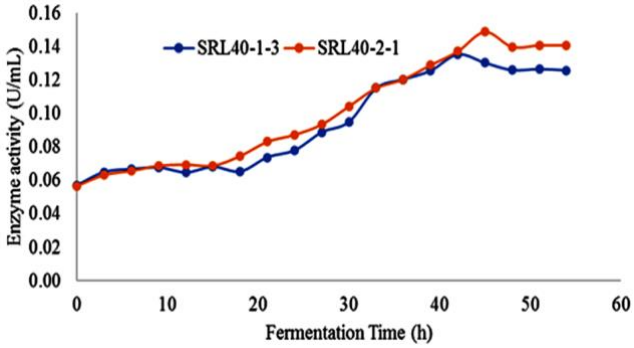


**Figure 5.** Determination of enzyme activity at the optimum fermentation time

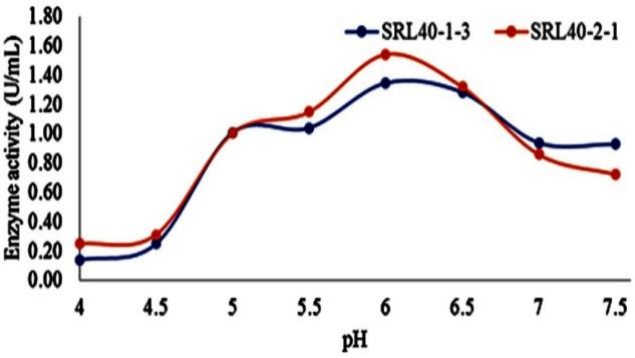


**Figure 6.** Effect of pH on enzyme activity

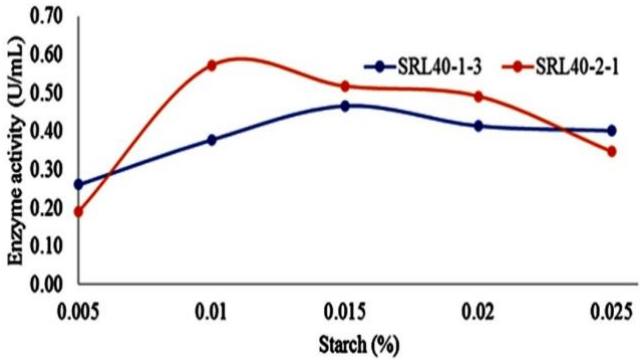


**Figure 7.** Effect of substrate concentration on enzyme activity

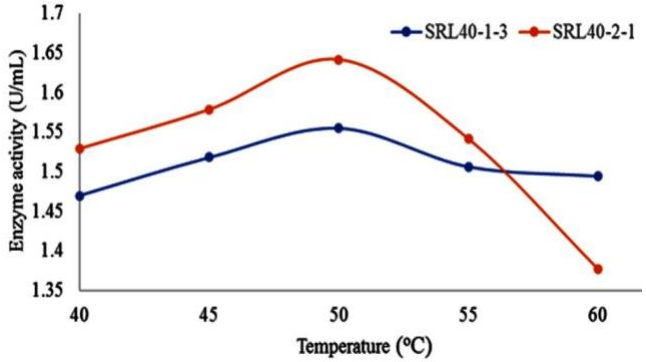


**Figure 8.** Effect of temperature on enzyme activity

The optimum concentration of rice in this study differs quite significantly from previous studies, such as the optimum starch concentration for each *B. licheniformis*, *B. cereus*, and *B. subtilis* was 1% (Bello et al. 2021), *E. hormaechei* 3%, *B. cereus* 3% (Arekemase et al. 2020). Beyond these doses, enzyme activity is expected to peak or decline due to substrate saturation, which occurs when all active sites are occupied.

*Effect of temperature on enzyme activity*

Figure 8 shows that the activity of the α-amylase enzyme in crude extracts increases with increasing temperature. Both SRL40-1-3 and SRL40-2-1 exhibit peak activity at 50°C, indicating that this temperature is optimal for catalytic efficiency. Temperature affects the activity of the α-amylase enzyme by altering the speed of molecular motion and the stability of its structure. At too low temperatures, the kinetic energy of the molecules decreases, reducing the frequency of collisions between the enzyme and the substrate and slowing the reaction rate. Conversely, at too high a temperature, the enzyme's three-dimensional structure can be disrupted by breaking non-covalent bonds, such as hydrogen bonds and hydrophobic interactions, leading to enzyme denaturation. When an enzyme is denatured, the shape of its active site changes, preventing it from binding specifically to its substrate and ultimately reducing or stopping enzyme activity (Farooq et al. 2021). An optimum temperature is needed for the enzyme to function optimally without losing its stability. The other studies showed the optimum temperature for *B. licheniformis* and *B. subtilis* was 65°C (Msarah et al. 2020), *A. oryzae* 55°C (Balakrishnan et al. 2021), *B. amyloliquefaciens* 45°C (Pham et al. 2021), and *Bacillus* sp. 50°C (Rajesh and Gummadi 2022). However, exceeding the temperature can cause reduced enzyme activity due to denaturation, a process in which the protein structure loses its functional conformation. This temperature-dependent response shows the isolates' thermophilic characteristics, which are conducive to elevated temperatures.

In conclusion, this study successfully identified two significant activity strains of amylase-producing bacteria. Isolates SRL40-1-3 and SRL40-2-1 showed high amylolytic activity, with SRL40-2-1 and SRL40-1-3 having a clear zone of 5.1 cm and 4.0 cm, respectively. The morphological results showed that SRL40-1-3 was spiral-shaped and SRL40-2-1 was coccoid-shaped. Both isolates were classified as Gram-positive bacteria with different morphologies. Furthermore, biochemical tests revealed metabolic differences, with only SRL40-1-3 demonstrating the potential to use citrate as a carbon source. In sugar media, both isolates showed the capacity to ferment. Molecular identification confirmed that both isolates belonged to the genus *Enterobacter*; SRL40-1-3 was *Enterobacter* sp., and SRL40-2-1 was *E. hormaechei*. The results showed that the starch level of sago waste was 19.73%, providing fresh opportunities for future applications. The optimum conditions for α-amylase production were 1.25% starch, 0.12% $CaCl_2$, 42 h for *Enterobacter* sp., and 0.75% starch, 0.08% $CaCl_2$, 45 h for *E. hormaechei*. Despite the significant contribution, this study had limitations, including the need to further purify the isolated α-amylase to achieve the required purity for biotechnological applications. Therefore, future studies should focus on further enzyme purification and on validating bioactivity through biotechnological applications such as bioenergy, food, and drink products, as well as their derivatives.

## ACKNOWLEDGEMENTS

The authors are grateful for the cooperation of all students and lecturers of the Doctoral Program, Department of Chemistry, Faculty of Mathematics and Natural Science, Universitas Hasanuddin, Indonesia. LPPM Universitas Hasanuddin supported this study through the PFK schema 2024 fiscal year program with contract No.00309/UN4.22/PT.01.03/2024.

## REFERENCES

Abd-Elaziz AM, Karam EA, Ghanem MM, Moharam ME, Kansoh AL. 2020. Production of a novel α-amylase by *Bacillus atrophaeus* NRC1 isolated from honey: Purification and characterization. Intl J Biol Macromol 148: 292-301. DOI: 10.1016/j.ijbiomac.2020.01.120.

Abdollahi P, Ghane M, Babaeekhou L. 2020. Isolation and characterization of thermophilic bacteria from Gavmesh Goli hot spring in Sabalan geothermal field, Iran: *Thermomonas hydrothermalis* and *Bacillus altitudinis* isolates as a potential source of thermostable protease. Geomicrobiol J 38: 87-95. DOI: 10.1080/01490451.2020.1812774.

Al-Agamy MH, Alhuzani MR, Kelany MS, Hamed MM. 2021. Production and partial characterization of α -amylase enzyme from marine actinomycetes. Biomed Res Intl 2021: 5289848. DOI: 10.1155/2021/5289848.

Al-Fakih GOA, Ilyas RA, Huzaifah MRM, El-Shafay AS. 2024. Recent advances in sago (*Metroxylon sagu*) fibres, biopolymers, biocomposites, and their prospective applications in industry: A comprehensive review. Intl J Biol Macromol 269 (Pt 1): 132045. DOI: 10.1016/j.ijbiomac.2024.132045.

Andriyani H, Natacia N, Fachrial E. 2021. Production of antimicrobial compounds using thermophilic bacteria species *Bacillus subtilis* and *Bacillus Tequilensis*. ITEGAM-JETIA J Eng Technol Ind Appl 7 (31): 18-25. DOI: 10.5935/jetia.v7i31.776.

Angio NM, Abdul A, Kumaji SS, Uno WD, Retnowati Y, Jannah M. 2024. Analysis of amylase activity in bacteria isolated from hot spring of Pentadio Resort. Jurnal Pembelajaran dan Biologi Nukleus 10 (1): 266-275. DOI: 10.36987/jpbn.v10i1.5506.

Arekemase MO, Alfa OP, Agbabiaka TO, Ajide-Bamigboye NT, Aderoboye OY, Orogu JO, Ahmed T. 2020. Optimization of amylase produced from bacteria isolated from cassava peel dumpsite using submerged fermentation. Sci World J 15: 64-75. DOI: 10.4314/swj.v15i1.

Arfah RA, Lestari YA, Dali S, Muliadi, Liestianty D. 2020. The isolation of *Termofil amilolitik* bacterium and activity test of harsh extract amylase enzyme from the hot spring at Jailolo Bay in North Maluku. J Phys: Conf Ser 1569: 042050. DOI: 10.1088/1742-6596/1569/4/042050.

Balakrishnan M, Jeevarathinam G, Kumar SKS, Muniraj I, Uthandi S. 2021. Optimization and scale-up of α-amylase production by *Aspergillus oryzae* using solid-state fermentation of edible oil cakes. BMC Biotechnol 21: 33. DOI: 10.1186/s12896-021-00686-7.

Bello AY, Abdulkadir N, Abubakar S, Lawal A. 2021. Studies on screening and optimization of amylase enzyme production using bacteria isolated from soil. J Microbiol Exp 9 (6): 196-200. DOI: 10.15406/jmen.2021.09.00343.

Benammar L, Bektaş Kİ, Menasria T, Beldüz AO, Güler HI, Bedaida IK, Gonzalez JM, Ayachi A. 2020. Diversity and enzymatic potential of thermophilic bacteria associated with terrestrial hot springs in Algeria. Braz J Microbiol 51 (4): 1987-2007. DOI: 10.1007/s42770-020-00376-0.

Bhatt K, Lal S, Srinivasan R, Joshi B. 2020. Bioconversion of agricultural wastes to produce α-amylase from *Bacillus velezensis* KB 2216: Purification and characterization. Biocatal Agric Biotechnol 28: 101703. DOI: 10.1016/j.bcab.2020.101703.

Boymurod Y. 2024. Microorganisms in nature, their shapes and sizes. Intl J Adv Sci Res 4 (5): 63-67. DOI: 10.37547/ijasr-04-05-13.

Budiharjo A, Wulandari D, Shabrina J, Mawarni RA, Maulana AR, Nurhayati, Wijanarka W, Hartajanie L, Lindayani. 2024. Bioprospecting and molecular identification of amylase and cellulase producing thermophilic bacteria from sediment of Nglimut Hot Springs, Kendal Regency. J Trop Biodivers Biotechnol 9 (3): jtbb86756. DOI: 10.22146/jtbb.86756.

Dalton L, Young R. 2024. Fundamentals of Cell Biology. Oregon State University, Corvallis, OR, USA. https://open.oregonstate.education/cellbiology.

Farooq MA, Ali S, Hassan A, Tahir HM, Mumtaz S, Mumtaz S. 2021. Biosynthesis and industrial applications of α-amylase: A review. Arch Microbiol 203: 1281-1292. DOI: 10.1007/s00203-020-02128-y.

Fazal BZ, Budiman C, Amin Z, Ling CMWV. 2022. Screening, isolation, and characterization of amylase-producing bacteria from Poring Hot Spring Sabah, Malaysia. Biodiversitas 23 (6): 2807-2815. DOI: 10.13057/biodiv/d230604.

Fetriyuna F, Letsoin SMA, Jati IRAP, Purwestri RC. 2024. Potential of underutilized sago for bioenergy uses. Intl J Adv Sci Eng Inform Technol 14 (1): 144-150. DOI: 10.18517/ijaseit.14.1.19202.

Fincan SA, Özdemir S, Karakaya A, Enez B, Mustafov SD, Ulutaş MS, Şen F. 2021. Purification and characterization of thermostable α-amylase produced from *Bacillus licheniformis* So-B3 and its potential in hydrolyzing raw starch. Life Sci 264: 118639. DOI: 10.1016/j.lfs.2020.118639.

Marzuki I, Kamaruddin M, Ahmad R. 2021. Identification of marine sponges-symbiotic bacteria and their application in degrading polycyclic aromatic hydrocarbons. Biodiversitas 22 (3): 1481-1488. DOI: 10.13057/biodiv/d220352.

Mittal A, Joshi M, Rath SK, Singh D, Dwibedi V. 2022. Isolation of alpha amylase-producing bacteria from local region of Ambala and production of amylase under optimized factors using solid-state fermentation. Curr Microbiol 79 (12): 375. DOI: 10.1007/s00284-022-03081-3.

Msarah MJ, Ibrahim I, Hamid AA, Aqma WS. 2020. Optimization and production of α-amylase from thermophilic *Bacillus* spp. and its application in food waste biodegradation. Heliyon 6 (6): e04183. DOI: 10.1016/j.heliyon.2020.e04183.

Paul B. 2023. Concatenated 16S rRNA sequence analysis improves bacterial taxonomy. F1000Res 11: 1530. DOI: 10.12688/f1000research.128320.3.

Paul JS, Beliya E, Tiwari S, Patel K, Gupta N, Jadhav SK. 2020. Production of biocatalyst α-amylase from agro-waste 'rice bran' by using *Bacillus tequilensis* TB5 and standardizing its production process. Biocatal Agric Biotechnol 26: 101648. DOI: 10.1016/j.bcab.2020.101648.

Pham VHT, Kim J, Shim J, Chang S, Chung W. 2021. Purification and characterization of strong simultaneous enzyme production of protease and α-Amylase from an extremophile-*Bacillus* sp. FW2 and its possibility in food waste degradation. Fermentation 8 (1): 12. DOI: 10.3390/fermentation8010012.

Bangar SP, Ashogbon AO, Singh A, Chaudhary V, Whiteside WS. 2022. Enzymatic modification of starch: A green approach for starch applications. Carbohydr Polym 287: 119265. DOI: 10.1016/j.carbpol.2022.119265.

Rajesh R, Gummadi SN. 2022. α-amylase and cellulase production by novel halotolerant *Bacillus* sp. PM06 isolated from sugarcane pressmud. Biotechnol Appl Biochem 69 (1): 149-159. DOI: 10.1002/bab.2091.

Rakaz MA, Hussien MO, Ibrahim HM. 2021. Isolation, extraction, purification, and molecular characterization for thermostable α-amylase from locally isolated *Bacillus* species in Sudan. Biochem Res Intl 2021: 6670380. DOI: 10.1155/2021/6670380.

Rasyid TH, Kusumawaty Y, Hadi S. 2020. The utilization of sago waste: Prospect and challenges. IOP Conf Ser: Earth Environ Sci 415: 012023. DOI: 10.1088/1755-1315/415/1/012023.

Shen H, Ge X, Zhang Q, Zhang X, Lu Y, Jiang H, Zhang G, Li W. 2022. Dielectric barrier discharge plasma improved the fine structure, physicochemical properties and digestibility of α-amylase enzymatic wheat starch. Innov Food Sci Emerg Technol 78: 102991. DOI: 10.1016/j.ifset.2022.102991.

Sidiq FF, Coles D, Hubbard C, Clark B, Frewer LJ. 2021. Sago and the indigenous peoples of Papua, Indonesia: A review. J Agric Appl Biol 2 (2): 138-149. DOI: 10.11594/jaab.02.02.08.

Singla D, Singh A, Dhull SB, Kumar P, Malik T, Kumar P. 2020. Taro starch: Isolation, morphology, modification and novel applications concern-A review. Intl J Biol Macromol 163: 1283-1290. DOI: 10.1016/j.ijbiomac.2020.07.093.

Susanto B, Tosuli YT, Adnan, Cahyadi, Nami H, Surjosatyo A, Alandro D, Nugroho AD, Rashyid MI, Muflikhun MA. 2024. Characterization of sago tree parts from Sentani, Papua, Indonesia for biomass energy utilization. Heliyon 10: e23993. DOI: 10.1016/j.heliyon.2024.e23993.

Ulucay O, Gormez A, Ozic C. 2022. Identification, characterization and hydrolase producing performance of thermophilic bacteria: geothermal hot springs in the eastern and southeastern Anatolia regions of Turkey. Antonie Van Leeuwenhoek 115 (2): 253-270. DOI: 10.1007/s10482-021-01678-5.

Wulan S. 2018. Sago as an environmentally sustainable food resource in the climate change era. J Environ Sci Sustain Dev 1 (1): 53-73. DOI: 10.7454/jessd.v1i1.22.

Yassin SN, Jiru TM, Indracanti M. 2021. Screening and characterization of thermostable amylase-producing bacteria isolated from soil samples of Afdera, Afar Region, and molecular detection of amylase-coding gene. Intl J Microbiol 2021: 5592885. DOI: 10.1155/2021/5592885.

Zhai Y, Li X, Bai Y, Jin Z, Svensson B. 2022. Maltogenic α-amylase hydrolysis of wheat starch granules: Mechanism and relation to starch retrogradation. Food Hydrocoll 124 (Part A): 107256. DOI: 10.1016/j.foodhyd.2021.107256.